Modelling and process development for gaseous separation with silicone-coated polymeric membranes

Jiang, Xin; Kumar, Ashwani

Publisher's version / Version de l'éditeur:
https://doi.org/10.1002/cjce.20018
Canadian Journal of Chemical Engineering, 86, April, pp. 151-159, 2008

Modelling and Process Development for Gaseous Separation with Silicone-Coated Polymeric Membranes

Xin Jiang and Ashwani Kumar*

Institute for Chemical Process and Environmental Technology, National Research Council of Canada, Building M-12, Montreal Road Campus, Ottawa, ON, Canada K1A 0R6

This paper proposes a permeance equation for vapour–permanent gas mixtures in a silicone-coated polymeric membrane. The equation was derived from the Arrhenius relationship by combining an apparent activation energy and interaction parameter. Accurate values of transmembrane flux were obtained by incorporating this proposed equation, which was dependent on temperature and feed composition. The equation parameters were correlated with the experimental data of eight mixtures consisting of hydrocarbons such as ethylene, ethane, propylene and propane with nitrogen covering a broad range of temperature and concentration. A numerical integration scheme was used for developing a crossflow model utilizing the above equation, which allowed the estimation of product properties including the membrane plasticization cases. The study also reports examples of implementation of this approach in potential industrial applications for the recovery of ethylene and propylene from nitrogen.

Cet article propose une équation de permeance pour les mélanges vapeur–permanents de gaz dans une membrane polymère enduite de silicone. L'équation a été dérivée du rapport d'Arrhenius en combinant une énergie d'activation et un paramètre apparents d'interaction. Des valeurs précises du flux de transmembrane ont été obtenues en incorporant cette équation proposée, qui dépendait de la composition en température et en alimentation. Les paramètres de l'équation ont été corrélés avec les données expérimentales de huit mélanges se composant des hydrocarbures tels que l'éthylène, l'éthane, le propylène et le propane avec de l'azote couvrant une large gamme de la température et de concentration. Un arrangement numérique d'intégration a été employé pour développer un modèle de croisement de flux utilisant l'équation ci-dessus, qui a permis l'évaluation des propriétés de produit comprenant les cas de plasticization de membrane. L'étude indique également des exemples d'exécution de cette approche dans des demandes industrielles potentielles de rétablissement d'éthylène et de propylène de l'azote.

Keywords: membrane separation, simulation, permeance equation, hydrocarbons, nitrogen

INTRODUCTION

Polymeric membrane-based processes for gaseous separation have successfully been applied in several industrial fields as standard units for many decades which benefit from lower capital and utility costs (Coker et al., 1998). For appropriate process design and optimization, many mathematical models have been developed to predict the performance of membrane modules from rigorous mass, momentum, and energy balances (Hinchliffe and Porter, 1997; Kaldis et al., 2000). In most published literature such as Mattiott and Sorensen (2003), Sridhar and Khan (1999), and Alpers et al. (1999), mathematical models described binary or multi-component mixtures in hollow fibre or spiral-wound modules with cocurrent, countercurrent, and crossflow contact patterns including permeate pressure build-up, concentration polarization, and permeate sweep. Pressure, composition, and temperature-dependent permeabilities or permeances were incorporated inside the models by ''succession of state'' and orthogonal collocation methods (Thundyil and Koros, 1997; Kaldis et al., 1998). However, permeabilities or permeances were usually assumed to be constant for diffusion-selective membrane materials in isothermal permeation as shown by Shindo et al. (1985), Pan (1986), and Tessendorf et al. (1999).

Pinnau and He (2004), and Lin et al. (2006) have reported that vapour permeabilities or permeances apparently depend on both temperature and feed composition of vapour–permanent mixtures for vapour-selective membrane materials. Simulta-

*Author to whom correspondence may be addressed.
E-mail address: ashwani.kumar@nrc-cnrc.gc.ca
Can. J. Chem. Eng. 86:151–159, 2008

DOI 10.1002/cjce.20018

neously weakly condensable and permanent components in the same mixtures could have coupling effects due to strong sorbing vapours, which swell polymer matrix (Jiang and Kumar, 2005, 2006). To design such membrane separation processes rationally, it is essential to calculate transmembrane flux precisely as the permeances are dependent on both temperature and feed composition in membrane modules. There are very few articles discussing permeance correlations with operating conditions that are based on actual experimental data. Merkel et al. (2000) correlated ten pure gas and vapour permeabilities with the pressure difference at 35°C for a filler-free polydimethylsiloxane (PDMS) film as follows:

$$Q = Q_0\{1 + b(P - p)\} \tag{1}$$

where Q_0 is the permeability coefficient at $P - p = 0$. The value of b principally shows the interplay of plasticization, hydrostatic pressure, and penetrant solubility. Liu et al. (2006) expressed semi-empirical correlations for propylene–nitrogen mixtures in poly(ether block amide) composite membrane for a range of 3–50°C:

Propylene :

$$J = \frac{D_0/\phi}{l(Px - py)}\{\exp(\phi\omega Px) - \exp(\phi\omega py)\} \tag{2}$$

Nitrogen :

$$J = \frac{D_0/\phi(1 - y)}{yl\{P(1 - x) - p(1 - y)\}}\{\exp(\phi\omega Px) - \exp(\phi\omega py)\} \tag{3}$$

where parameters D_0/ϕ and $\phi\omega$ reflect intrinsic membrane characteristics for these two gases. However, these parameters reported by Liu et al. (2006) do not proportionally vary with temperature. Nitsche et al. (1998) expressed the permeances of pure propane, n-butane, n-pentane, and n-hexane for a typical PDMS composite membrane with the following equation:

$$J = J_0 \exp\left\{-\frac{E_p}{RT} + b_0 P \exp(b_1 T)\right\} \tag{4}$$

By using Equation (4), it is possible to calculate the permeances on the basis of Free Volume Model for a vapour–permanent gas mixture. However, in the case of commercial membranes such as reported in the present work, the free volume data are not easily available. Therefore, we have followed an approach to describe the permeation of low hydrocarbon and nitrogen mixtures mathematically for a silicone-coated composite membrane. First the composition and temperature-dependent permeance expression was derived from the Arrhenius relationship to achieve accurate transmembrane flux. The parameters in the expression were determined by non-linear regression (Marquardt-Levenberg routine) of experimental data from eight different mixtures consisted of nitrogen, ethylene, ethane, propylene, and propane in a temperature range from −14 to 23°C for the pressures of 384–400 kPa (a) with 1.0–28.0% (mol) total hydrocarbon concentration in feed. Secondly, a straightforward crossflow model was developed for membrane, which permitted the incorporation of this equation. This procedure allowed a rational simulation of a membrane process with real operating conditions for industrially important separations of ethylene–nitrogen and propylene–nitrogen.

MATHEMATICAL MODEL

Permeance

According to solution-diffusion approach, permeance, J, including vapours and permanent gases in a mixture are ordinarily expressed as shown by Leemann et al. (1996) as:

$$J = \frac{DG}{l} \tag{5}$$

Also, temperature-dependent diffusivity D and sorption coefficient G follow the Arrhenius relationship as described below:

$$D = D_0 \exp\left(\frac{-E_\mathrm{d}}{\mathrm{RT}}\right) \tag{6}$$

$$G = G_0 \exp\left(\frac{-\Delta h_\mathrm{s}}{\mathrm{RT}}\right) \tag{7}$$

Combining Equations (5), (6), and (7), the permeance can be expressed as:

$$J = J_0 \exp\left(\frac{-E_\mathrm{p}}{RT}\right) \tag{8}$$

$$J_0 = \frac{D_0 G_0}{l} \tag{9}$$

$$E_\mathrm{p} = E_\mathrm{d} + \Delta h_\mathrm{s} \tag{10}$$

where E_p refers as apparent activation energy including activation energy for a diffusion step E_d and the heat of sorption Δh_s.

The selectivity for a pair of gases in a mixture is:

$$S_{ij} = \frac{J_i}{J_j} \tag{11}$$

For vapour-selective membrane materials, the permeances for a vapour–permanent gas mixtures strongly depend on the temperature and feed composition (Pinnau and He (2004) and Jiang and Kumar (2005)). Moreover, we noted (Jiang and Kumar, 2006) that the E_p of hydrocarbon is also influenced by its feed concentration in addition to the physical properties of the penetrant and polymer matrix as well as the chemical structure of the polymer. Due to the coupling effect, the E_p of permanent gas in the same mixture is affected by total feed hydrocarbon concentration at varying operating temperatures to a different extent. For hydrocarbon and nitrogen mixtures in the present study, these could be described by first-order polynomial expressions as:

$$\text{Hydrocarbon(s)}: \quad E_{\mathrm{p},i} = E_i(1 + B_i T x_i) \tag{12}$$

$$\text{Nitrogen}: \quad E_{\mathrm{p,N2}} = E_{\mathrm{N2}}(1 + B_{\mathrm{N2}} T x_t) \tag{13}$$

Substituting Equations (12) and (13) into (8), and assuming $a_i = -\frac{B_i E_i}{R}$ and $a_{\mathrm{N2}} = -\frac{B_{\mathrm{N2}} E_{\mathrm{N2}}}{R}$, hydrocarbon permeances in a mixture were represented as follows:

$$J_i = J_{0,i} \exp\left(\frac{-E_i}{RT} + a_i x_i\right) \tag{14}$$

The exception was nitrogen where:

$$J_{N2} = J_{0,N2} \exp\left(\frac{-E_{N2}}{RT} + a_{N2}x_t\right) \quad (15)$$

For each component in a mixture, J_0 refers to the permeance when temperature T is extremely high and feed concentration x approaches zero. Apparent activation energy E principally indicates that it is an endothermic permeation process (positive) or an exothermic permeation process (negative). Theoretically, permeance increases with decreasing temperature in an exothermic permeation process, conversely permeance decreases with decreasing temperature in an endothermic permeation process. Apparent interaction parameter ''a'' shows sensitivity to the feed concentration quantitatively due to the fact that the membrane was plasticized by sorbing penetrant(s) to a different degree of swelling. The values of J_0, E and ''a'' can be obtained through the Marquardt-Levenberg algorithm for non-linear regression using experimental data on the transmembrane flux at various feed concentrations, temperatures, and pressures. Calculated J_i and J_{N2} principally are independent of the operating pressure as will be discussed later in the Section ''Error Analysis.''

Table 1 lists all parameters of Equations (14) and (15) for eight different mixtures using same membrane and experimental set-up as described in our previous work (Jiang and Kumar, 2006). Most multiple correlation coefficients ($R1$) were near 1, indicating that the equations were good descriptions of the relations between the independent and dependent variables. The probabilities of being wrong (PW) in concluding that the fitted parameters are not zero were less than 0.05 in most cases. Therefore the independent variables (T, x_i and x_t) can be used to predict the dependent variables (J_i and J_{N2}) without significant errors. Coincidently with experimental results reported earlier (Jiang and Kumar, 2006), the E-values of propylene and propane were always negative in the mixtures containing propylene, propane, or both. This implies that these strong sorbing penetrants loosened segmental chains in the polymeric matrix. Moreover, ''a'' values of both propylene and propane increased considerably with the increase of the component number for a mixture, showing that $C_2^=$ Quaternary and C_2 Quaternary mixtures plasticized PDMS coating to the highest degree of swelling in the mixtures including C_3 ternary, $C_3^=$ binary and C_3 binary. This can also be confirmed from E and ''a'' values of ethylene and ethane in these two mixtures compared with other mixtures containing no propylene and/or propane. For example, ''a'' values of ethylene and ethane in the mixtures of $C_2^=$ Quaternary and C_2 Quaternary were much higher than those in the mixtures of $C_2^=$ Binary, C_2 Binary, and C_2 Ternary due to strong coupling effects. Simultaneously their E-values became negative, indicating that ethylene and ethane were in exothermic permeation processes in the presence of C_3 components. Based on the positive E-values, it can be concluded that there was no plasticization for $C_2^=$ Binary and C_2 Binary mixtures, and slight plasticization occurred for C_2 Ternary mixture since only ethane E was negative and closed to zero. Also, nitrogen E and ''a'' values in all eight mixtures showed an endothermic permeation process. However, its permeances were significantly impacted by the swelling degrees which were demonstrated by the magnitudes of ''a'' values, indicating that the nitrogen permeances were elevated adequately in a larger ''a'' value gas mixtures. So, it appears that nitrogen ''a'' values in the mixtures of $C_3^=$ Binary, C_3 Binary, and C_3 Ternary were much larger than those in the mixtures of $C_2^=$ Binary, C_2 Binary, and C_2 Ternary. It is interesting to note that nitrogen ''a'' values in the mixtures of $C_2^=$ Quaternary and C_2

Table 1. Parameters in Equations (14) and (15) for eight mixtures.

Mixture	Component	J_0, GPU	E, J/mol	a	R_1
$C_2^=$ Binary	N_2	24 013	11 863	0.13	0.994
	C_2H_4	23 186	7385	0.89	0.951
C_2 Binary	N_2	24 786	12 207	0.12*	0.990
	C_2H_6	2790	2086	1.21	0.914
C_2 Ternary	N_2	17 278	11 409	0.16	0.995
	C_2H_4	2272	2428	3.18	0.905
	C_2H_6	839	−814	2.62	0.928
$C_3^=$ Binary	N_2	7801	9529	0.87	0.988
	C_3H_6	373	−3153	2.09	0.917
C_3 Binary	N_2	5252	8561	0.97	0.977
	C_3H_8	87	−6579	3.07	0.925
C_3 Ternary	N_2	6586	9114	0.84	0.982
	C_3H_6	565	−2144	5.01	0.928
	C_3H_8	145	−5531	6.40	0.937
$C_2^=$ Quaternary	N_2	9213	9899	0.58	0.990
	C_2H_4	571	−1088*	6.97	0.925
	C_3H_6	443	−2557	9.17	0.900
	C_3H_8	235	−4666	6.96	0.894
C_2 Quaternary	N_2	8009	9516	0.48	0.988
	C_2H_6	444	−1993	6.95	0.862
	C_3H_6	652*	−1690*	8.46	0.856
	C_3H_8	224	−4678	7.39	0.912

Operational range: temperature, from −14 to 23°C; feed pressure, 384–400 kPa (a); total hydrocarbon concentration in feed, 1.0–28.0% (mol). Stage cuts were less than 0.012. *PW were larger than 0.05.

Quaternary were even smaller than those in the mixture of $C_3^=$ Binary, C_3 Binary, and C_3 Ternary. This is due to the fact that weakly condensable ethylene or ethane in the same mixtures competed for the limited activated sites. Choosing $C_3^=$ Binary and $C_2^=$ Binary mixtures as examples, Figures 1 and 2 show the distinction between plasticization and no-plasticization permeance and selectivity with calculated and experimental data at varying temperatures and feed concentrations.

Membrane Process

The spiral wound membrane module consists of many flat membrane envelopes, which are wrapped around a central pipe with fluid-conductive spacers inside and outside envelopes. The feed under high pressure is introduced from one end of the shell-side. As feed gas passes along the length of the membrane module, a portion of feed gas as permeate penetrates into the membrane envelopes with low pressure. It travels perpendicularly to the feed and spirals to a central collecting pipe. The rest of the feed gas leaves at another end of the shell-side as residue. Figure 3 shows the diagram of a flat membrane envelope with the flow configuration and the computational scheme. The numerical integration was adopted for modelling the separation of multi-component mixtures, which permitted the incorporation of pressure, composition, and temperature-dependent permeances as represented by Coker et al. (1998) and Thundyil and Koros (1997). The membrane envelopes were divided into a series of N sections in the axial direction of the central pipe. Boundary conditions included feed composition, feed flow-rate and pressure, permeate pressure, and operating temperature. Following assumptions were made for formulating the numerical models:

1. Gas flows were at steady state in the membrane at isothermal conditions.
2. The deformation of membrane under pressure was negligible.
3. There was no gas mixing of shell and permeate sides in the directions of bulk flows.
4. The pressure build-up in shell and permeate sides were negligible.
5. Feed composition change in any selected infinitely small section k was ignored.

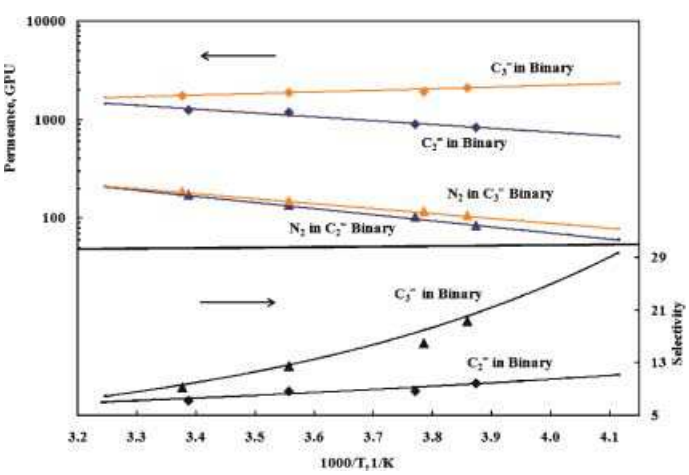

Figure 1. Comparison of calculated and experimental data of permeance and selectivity as the function of temperature for $C_2^=$ Binary and $C_3^=$ Binary. Lines and symbols represent calculated and experimental data, respectively. Feed pressure: 394 ± 2 kPa (a). Permeate pressure: 101.3 kPa (a). Feed composition: 87% nitrogen, 13% ethylene for $C_2^=$ Binary; 87% nitrogen and 13% propylene for $C_3^=$ Binary.

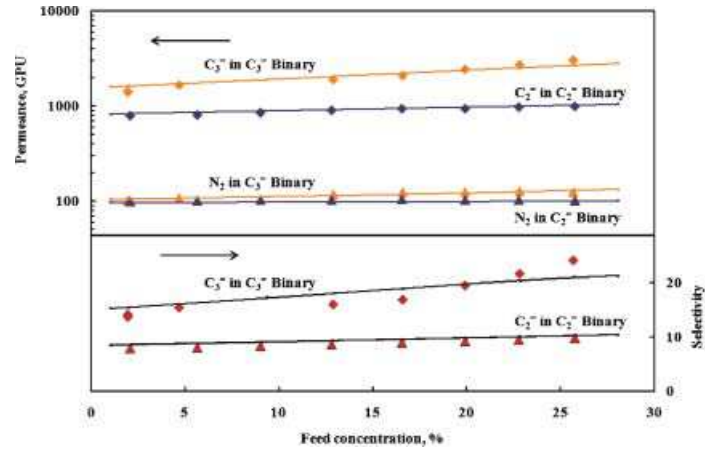

Figure 2. Comparison of calculated and experimental data of permeance and selectivity as the function of hydrocarbon concentration in feed for $C_2^=$ Binary and $C_3^=$ Binary. Lines and symbols represent calculated and experimental data, respectively. Feed pressure: 393 kPa (a). Permeate pressure: 101.0 kPa (a). Temperature: $-8°C$.

In each section, component i transmembrane flux of a mixture from feed to permeate sides across the membrane was described by Ghosal and Freeman (1994) as:

$$v_k y_{k,i} = J_i \Delta A (P x_{k-1,i} - p y_{k,i}) \tag{16}$$

where

$$\Delta A = 2mW\Delta L = \frac{2mWL}{N},$$

v_k and $y_{k,i}$ are the mass flow-rate and concentration of component i that leaves the membrane skin surface in section k. According to Equation (16) concentration $y_{k,i}$ principally depends on the permeance, feed concentration, feed and permeate pressures. Therefore, the composition of this transmembrane flux does not relate with any other gas flow-rates which are obtained by the permeation in adjacent sections on the permeate side. Equation (16) can be rewritten as:

$$y_{k,i} = \frac{J_i \Delta A P x_i}{v_k + J_i \Delta A p} \tag{17}$$

In this model, the permeances for each component in this section were determined by the operating temperature and feed composition located at section $k-1$ using Equations (14) and (15), then composition and temperature-dependent permeances were placed into the model.

To obtain the value of $y_{k,i}$, initially v_k was set to zero and then checked if $\sum_{i=1}^{n} y_{k,i} = 1$. This procedure was iterated by an increment of v_k until the inequality $|\sum_{i=1}^{n} y_{k,i} - 1| \leq 0.0002$ was satisfied. These v_k and $y_{k,i}$ values were the transmembrane flux and their concentrations produced by the permeation in section k.

According to the mass balance for section k, the flow-rates and compositions of both permeate and residue streams were obtained as follows:

$$V_k = V_{k-1} + v_k \tag{18}$$

$$Y_{k,i} = \frac{V_{k-1} Y_{k-1,i} + v_k y_{k,i}}{V_k} \tag{19}$$

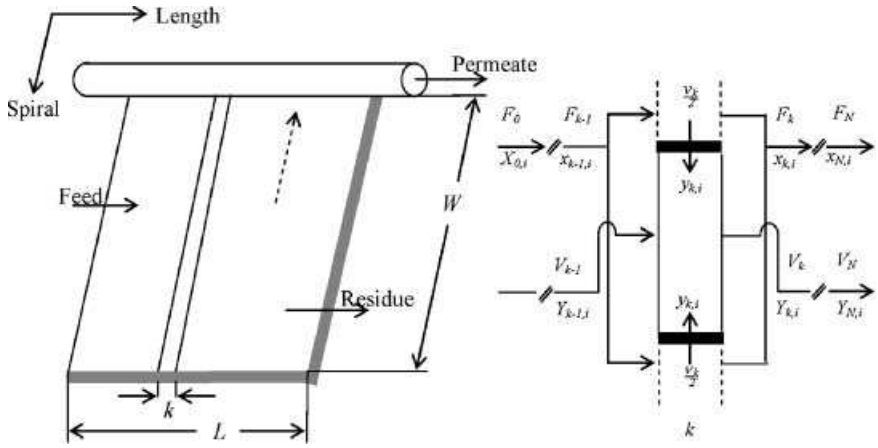

Figure 3. One flat membrane envelope in spiral wound module and the computational scheme.

$$F_k = F_{k-1} - v_k \tag{20}$$

$$x_{k,i} = \frac{F_{k-1}x_{k-1,i} - v_k y_{k,i}}{F_k} \tag{21}$$

Applying this straightforward crossflow model in series from *1* to *N* section with given boundary conditions at feed, the profiles of feed flow-rate and composition along the axial direction were obtained, which naturally showed the permeance variations in each section. At the end, the compositions and flow-rates of permeate and residue, located at section *N*, were calculated accurately for a large membrane area to be used in a module.

The membrane process in this paper refers to only membrane modules. It can be module-in-series, module-in-parallel, or a combination as described by Baker et al., (1998). This arrangement depends on the optimum design required for a particular application. Finally, the total recovery of hydrocarbon *i* for whole membrane process was represented as:

$$Rp_i = \frac{V_T Y_{T,i}}{FoXo_i} \tag{22}$$

MODEL ASSESSMENT

Error Analysis

As presented above, this numerical integration scheme is the approximation of differential equations as transmembrane flux of each section is determined by the input conditions of the section and, therefore, simulation accuracy strongly depends on section size. The decrease of section size (i.e., increase of *N* number) can reach asymptotic values, demonstrating that the simulation accuracy is within acceptable limits. Usually product properties are chosen to evaluate the simulation accuracy. In our approach, the hydrocarbon concentrations and recoveries of permeate were used to test the accuracy. Two gaseous mixtures (experimental conditions in Table 2) representing plasticization ($C_3^=$ Binary) and no-plasticization ($C_2^=$ Binary) conditions were selected to illustrate the relationship between the section number and product properties for a large membrane area suitable for a module as depicted in Figure 4. As expected, ethylene and propylene concentrations and recoveries in permeate were approaching the asymptotic values, but they did not attain asymptotic values immediately even at $N = 10$. These product properties at $N = 50$ were presumably very close to asymptotic values. The errors of the product properties at $N = 40$ compared to those at $N = 50$ were less than 0.13%. As a consequence of above analysis, $N = 40$ was used in later simulations for an 8 m^2 membrane area. Also, simulation accuracy of the model was evaluated by experimental results. Figure 5 shows the effect of operating pressure on calculated and experimental data for $C_2^=$ Binary and $C_3^=$ Binary mixtures. The errors between calculated and experimental data were not significant at higher operating pressure, indicating that *Ji* and J_{N2} values of Equations (14) and (15) obtained from a fixed operating pressure can be used to predict the product properties of a membrane process at other operating pressures. Specifically, this modelling technique not only works for both plasticization and no-plasticization permeation behaviours but also for different operating pressures. It will be further verified in the following examples relevant for industrial applications that these equations would be applicable under different process conditions.

Ethylene Recovery

Figures 6 and 7 show an ethylene recovery process from the feed stream of 20% ethylene, 5% ethane, and 75% nitrogen (C_2 Ternary) which has no significant membrane plasticization as mentioned in the Section ''Permeance.'' This membrane process had a module-in-series, and was designed to achieve greater than 95% recovery of ethylene and ethane in permeate (product recovery) and 99% nitrogen purity in residue. It can be seen clearly from Figure 6 that the required membrane area apparently decreases with increasing

Table 2. Operating conditions for the data presented in Figure 4.

	$C_3^=$ Binary	$C_2^=$ Binary
Feed flow-rate	400 Nm^3/h	400 Nm^3/h
Feed pressure	1.45 MPa (a)	2.16 MPa (a)
Permeate pressure	0.12 MPa (a)	0.12 MPa (a)
Feed composition	20% propylene 80% nitrogen	20% ethylene 80% nitrogen
Temperature	−10°C	10°C
Membrane area	8 m^2 (four envelopes)	8 m^2 (four envelopes)
Module size	Φ 100 × 1000 mm	Φ 100 × 1000 mm

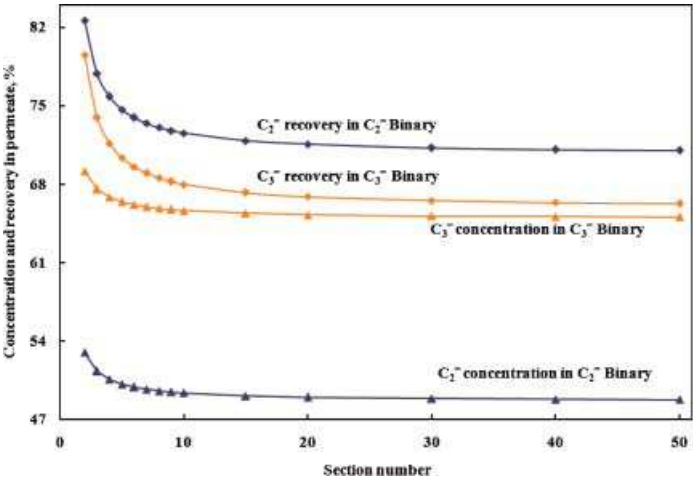

Figure 4. Evaluation of simulation accuracy for the mathematical model of membrane modules. Operating conditions are given in Table 2.

temperature from −40°C to 30°C, matching positive *E*-values of both ethylene and nitrogen in Equations (14) and (15). That is, their permeances increased with the increase of temperature except for ethane. However, ethylene or ethane selectivities to nitrogen might decrease slightly with the increase of temperature. As a result, the concentrations of ethylene and ethane in permeate (product purities) was reduced by approximately 32% for a 70°C difference. For example, ethylene concentration in permeate was decreased from 41.7% to 28.7%. Also, the elevation of feed operating pressure reduced the required membrane areas without the obvious influence to ethylene and ethane concentrations in permeate as shown in Figure 7. This occurs when the selectivity and pressure ratio between feed and permeate have similar values (Baker and Wijmans, 1994). So, when this membrane process would be implemented in a polyethylene de-gassing operation, nitrogen recycles to the reactor directly, and C_2 products can be fed to the cooling system for further purification. A substantial saving of membrane area will result under higher operating temperature and pressure.

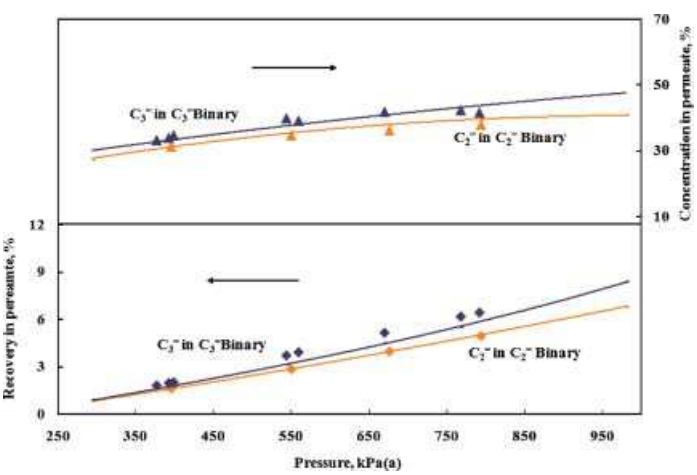

Figure 5. The effect of operating pressure on concentration and recovery in permeate for $C_2^=$ Binary and $C_3^=$ Binary. Lines and symbols represent calculated and experimental data, respectively. $C_2^=$ Binary feed flow-rate: 0.345Nm^3/h; feed composition: 87% nitrogen, 13% ethylene; temperature: 22°C. $C_3^=$ Binary feed flow-rate: 0.348 Nm^3/h; feed composition: 87% nitrogen, 13% propylene; Temperature: 30°C. All permeate pressure: 101.0kPa (a) and membrane area: 10.5×10^{-4} m^2.

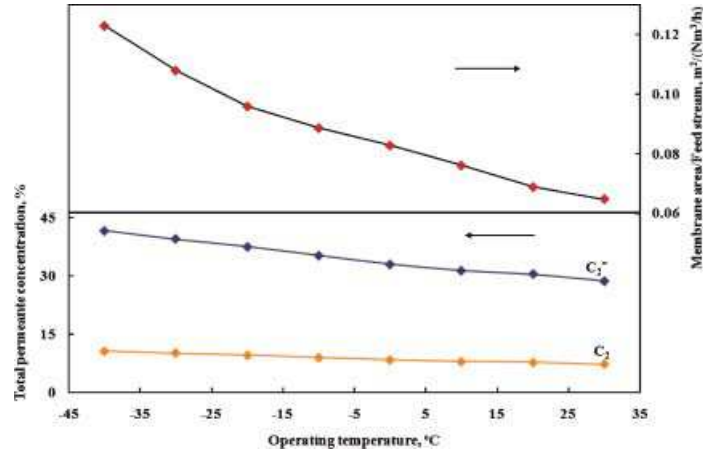

Figure 6. Effect of operating temperature on membrane area and product purity for C_2 Ternary with 95% product recovery and 98% nitrogen in residue. Feed flow-rate: 500 Nm^3/h. Feed composition: 20% ethylene, 5% ethane, and 75% nitrogen. Feed pressure: 1.57 MPa (a). Permeate pressure: 0.15 MPa (a).

Also the effect of membrane area and feed concentrations on product purity and recovery for ethylene–nitrogen ($C_2^=$Binary) at 20°C are represented in Figure 8. Ethylene concentration and recovery in permeate followed a trade-off relationship as the membrane area changed. The higher recovery caused a lower hydrocarbon concentration in permeate (Coker et al., 1998; Liu et al., 2006). Higher ethylene concentration in the feed stream produced higher permeate concentration and recovery because of higher partial pressure differences between feed and permeate sides at a fixed membrane area.

Propylene Recovery

Similarly, Figures 9 and 10 show a propylene recovery process from the feed stream of 15% propylene, 5% propone, and 85 % nitrogen (C_3 Ternary) with significant membrane plasticization as mentioned in the Section ''Permeance.'' Again, the membrane process was a module-in-series, and was designed to achieve greater than 93% recovery of propylene and propane in permeate (product recovery) and greater than 98% nitrogen purity in the

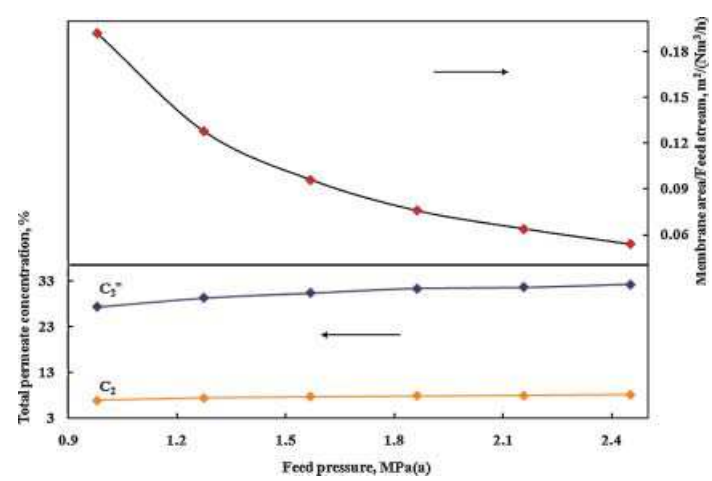

Figure 7. Effect of feed pressure on membrane area and product purity for C_2 Ternary with 98% product recovery and 99% nitrogen in residue. Feed flow-rate: 500 Nm^3/h. Feed composition: 20% ethylene, 5% ethane, and 75% nitrogen. Temperature: 0°C. Permeate pressure: 0.15 MPa (a).

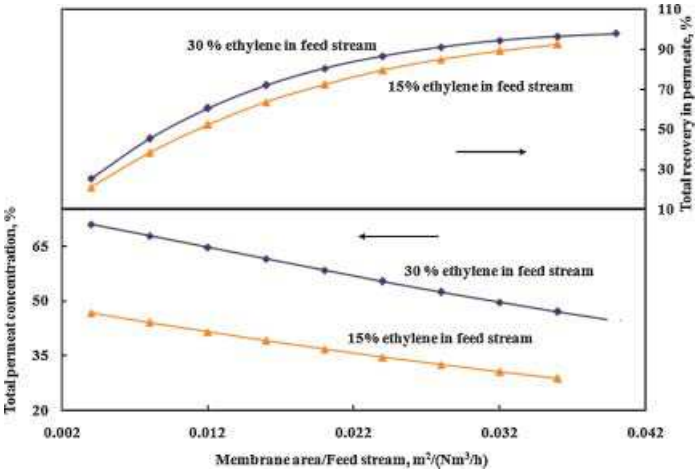

Figure 8. Effect of membrane area on total ethylene concentration and recovery in permeate for $C_2^=$Binary at two feed compositions. Feed flow-rate: 500 Nm^3/h. Temperature: 20°C. Feed pressure: 2.16 MPa (a). Permeate pressure: 0.15 MPa (a).

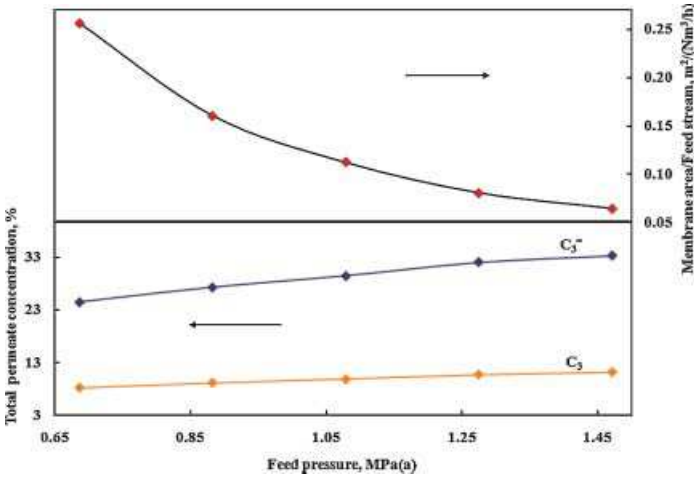

Figure 10. Effect of feed pressure on membrane area and product purity for C_3 Ternary with 95% product recovery and 98% nitrogen in residue. Feed flow-rate: 500 Nm^3/h. Feed composition: 15% propylene, 5% propane, and 80% nitrogen. Temperature: −10°C. Permeate pressure: 0.15 MPa (a).

residue. It is clear from Figure 9 that the concentrations of propylene and propane in permeate (product purities) reduced by 37.1% and 28.0%, respectively, as temperature was increased from −25°C to 30°C, indicating that propylene and propane selectivities to nitrogen decreased significantly during this 55°C difference. This is due to the negative *E*-values of propylene and propane and positive *E*-value of nitrogen (see Table 2), showing the opposite permeance propensities between C_3 components and nitrogen toward temperature change. In contrast to ethylene recovery process, increasing the temperature reduced the required membrane areas slightly from 0.064 to 0.052 $m^2/(Nm^3/h)$. In addition, elevating the feed operating pressure always diminishes the required membrane areas by increasing the driving force between feed and permeate sides. In this case, it also upgraded the propylene purities from 24.5% to 33.3% for an isothermal permeation. However, propane purities only increased from 8.16% to 11.2%, implying that feed concentration did impact the permeation as described in Equation (14) even though propane is the strongest swelling agent amongst these gases (see Figure 10). Comparing the membrane processes of propylene recovery and ethylene recovery, plasticization affects the performance of gas permeation remarkably in terms of membrane area, operating temperate, and pressure ratio. Also, the product purity and recovery as a function of membrane area and the composition of the feed stream were investigated by using two compositions of propylene–nitrogen mixtures (C_3 Binary) as illustrated in Figure 11. Propylene concentration and recovery in permeate not only represented the trade-off relationship for these two compositions but also strongly depended on its concentration in the feed stream. A higher propylene concentration in the feed stream enabled purer propylene and higher recovery in permeate. Summarizing the above simulation results with plasticization, the combination of membrane process with the condensation system would be more efficient for vapour–permanent gas separation by vapour-selective membrane. Liquefied hydrocarbons can be obtained by condensation of hydrocarbon-enriched permeate stream. Nitrogen can be

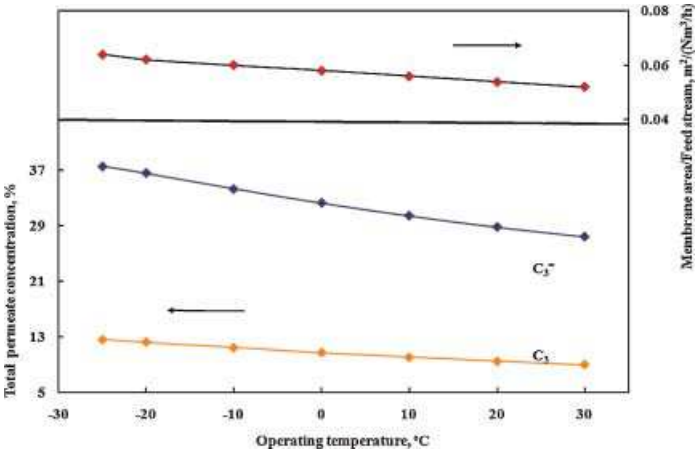

Figure 9. Effect of operating temperature on membrane area and product purity for C_3 Ternary with 93% product recovery and 98% nitrogen in residue. Feed flow-rate: 500 Nm^3/h. Feed composition: 15% propylene, 5% propane, and 80% nitrogen. Feed pressure: 1.47 MPa (a). Permeate pressure: 0.15 MPa (a).

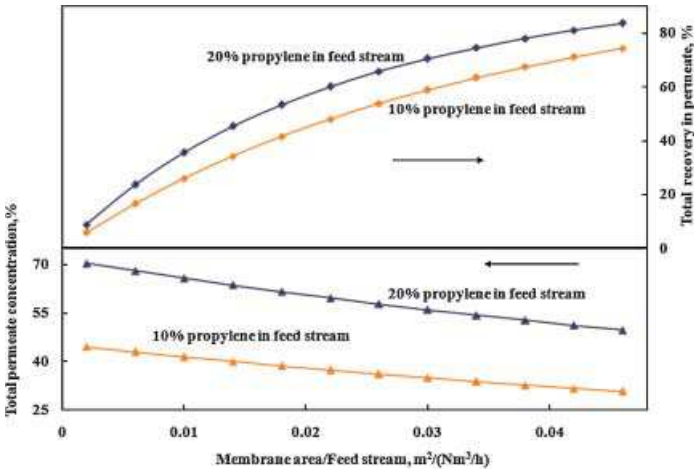

Figure 11. Effect of membrane area on total propylene concentration and recovery in permeate for $C_3^=$Binary at two feed compositions. Feed flow-rate: 500 Nm^3/h. Temperature: 0°C. Feed pressure: 1.27 MPa (a). Permeate pressure: 0.15 MPa (a).

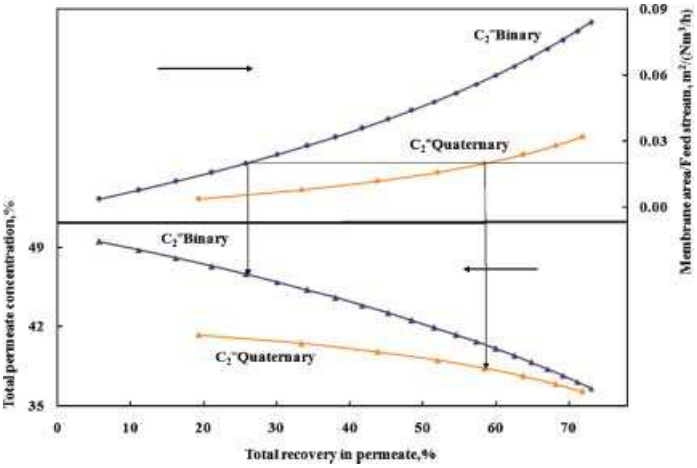

Figure 12. Comparison of ethylene in $C_2^=$ Binary and $C_2^=$ Quaternary for isothermal permeation. Temperature: −20°C. Feed pressure: 1.18 MPa (a). Permeate pressure: 0.15 MPa (a). $C_2^=$ Binary feed composition: 15% ethylene and 85% nitrogen. $C_2^=$ Quaternary feed composition: 15% ethylene, 7.5 percent propylene, 7.5% propane, and 70% nitrogen. Both feed flow-rate: 500 Nm^3/h.

reused from the residue of membrane process directly. The performance of the membrane process at sub-ambient temperature can give superior separation under moderate pressure differences between feed and permeate.

Plasticization Effect

As described above, plasticization significantly influences product properties with operating conditions. So, it is necessary to investigate the same penetrant in the membrane processes with the cases of plasticization and no-plasticization. Figure 12 shows ethylene permeation behaviours with the same concentrations of the feed streams in $C_2^=$ Binary and $C_2^=$ Quaternary at −20°C and a fixed ratio of feed and permeate pressures. Generally in membrane gas separation processes, the trade-off relationships for ethylene were represented by the recoveries and concentrations in permeate, and increasing the membrane area gave higher ethylene recoveries for both mixtures. Also, comparing these two mixtures, plasticization significantly enhanced the efficiency of separation for ethylene, which translated into higher recovery at a fixed membrane area or lower membrane area at a fixed recovery. For example, ethylene concentration and recovery were 47.0% and 26.1% in $C_2^=$ Binary; 38.7% and 58.6% in $C_2^=$ Quaternary at 0.02 $m^2/(Nm^3/h)$ membrane area/feed volume. On the other hand, ethylene concentration and membrane area/feed volume were 41.2% and 0.057 $m^2/(Nm^3/h)$ in $C_2^=$ Binary; 38.7% and 0.02 $m^2/(Nm^3/h)$ in $C_2^=$ Quaternary at 58.6% ethylene recovery. This separation efficiency definitely could be attributed to higher ethylene permeances and selectivities of $C_2^=$ Quaternary compared with those of $C_2^=$ Binary as illustrated in Figure 13. However, ethylene performance (purity and recovery in permeate) for $C2^=$ Quaternary was obviously lower than that for $C_2^=$ Binary with these superior membrane properties (permeance and selectivity, see Figure 12), resulting in lower ethylene concentration in permeate at a fixed recovery or membrane area. This was due to the fact that ethylene had to compete for the limited activated sites with stronger swelling agents (propylene and propane) in the same mixture. Incidentally, this typical comparison for the function of plasticization confirms the importance of ''a'' values in Equations (14) and (15) from another angle.

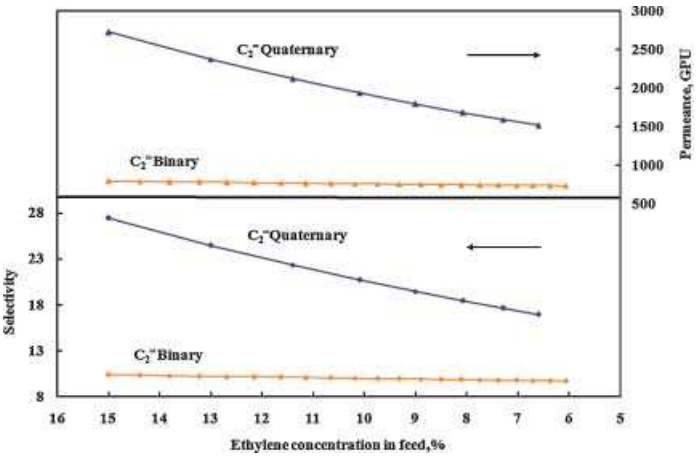

Figure 13. Ethylene permeance and selectivity as the function of its feed concentration for $C_2^=$ Binary and $C_2^=$ Quaternary in isothermal permeation (The conditions were as same as those given in Figure 12).

CONCLUSIONS

The proposed permeance equation correlated apparent activation energy and interaction parameter. The sign of apparent activation energy indicated the presence of plasticization or no-plasticization, while the values of interaction parameters quantified their effects. Using numerical integration method a straightforward crossflow model for membranes was developed, which predicted the permeate composition and recoveries at different operating pressures, adequately. For the separation of ethylene and ethane from nitrogen where no significant plasticization was present, increasing the temperature reduced the required membrane area considerably at a fixed recovery. For the separation of propylene and propane from nitrogen where significant plasticization was occurring, increasing temperature required comparable membrane area at a fixed recovery. It was concluded that in both cases the product properties strongly depended on hydrocarbon concentrations in feed stream. It was also shown that plasticization significantly enhanced the efficiency of separation for weakly condensable gas such as ethylene in the same mixture, which resulted in higher recovery at a fixed membrane area or lower membrane area at a fixed recovery.

ACKNOWLEDGEMENTS

Financial support from Natural Resources Canada under the HEIST-PERD program is gratefully acknowledged.

NOMENCLATURE

a	apparent interaction parameter in Equations (14) and (15)
A	effective membrane area, m^2
D	diffusion coefficient in Equations (5) and (6)
D_0	diffusion coefficient at very high temperature in Equation (6)
G	sorption coefficient in Equations (5) and (7)
G_0	sorption coefficient at very high temperature in Equation (7)
Δh_s	the heat of sorption in Equation (7), J/mol
E	apparent activation energy in Equations (12) to (15), J/mol
E_d	activation energy for a diffusion step in Equation (6), J/mol
E_p	apparent activation energy in Equation (8), J/mol

F	feed flow-rate in membrane process, Nm^3/h
Fo	the flow-rate of feed stream to membrane process, Nm^3/h
J_0	coefficient in Equations (8), (14), and (15), GPU (1 GPU = 10^{-6} cm^3 (STP)/$cm^2 \cdot s \cdot cmHg$)
J	permeance, GPU
l	membrane thickness
L	effective membrane length, m
m	membrane envelope number
n	component number in a mixture
N	section number
p	permeate pressure, kPa
P	feed pressure, kPa
PW	probability of being wrong in concluding that the parameter is not zero
R	idea gas constant (8.3145), J/(g-mol K)
R_1	multiple correlation coefficient
Rp	total recovery in permeate, %
t	temperature, ^oC
T	temperature, K
S	selectivity
v	transmembrane flux across a section, Nm^3/h
V	permeate flow-rate of membrane process, Nm^3/h
V_T	total permeate flow-rate of a membrane process, Nm^3/h
W	effective membrane width, m
x	feed molar fraction in F
Xo	concentration in feed stream F_0, mol %
y	permeate molar fraction leaving membrane surface
Y	permeate concentration in V, mol %
Y_T	total permeate concentration in V_T, mol %

Subscripts

i	component i
k	section k
t	total hydrocarbon concentration

REFERENCES

Alpers, A., B. Keil, O. Ludtke and K. Ohlrogge, ''Organic Vapor Separation: Process Design with Regards to High-Flux Membrane and the Dependence on Real Gas Behavior at High Pressure Applications,'' Ind. Eng. Chem. Res. **38**, 3745–3760 (1999).

Baker, R. W. and J. G. Wijmans, ''Membrane Separation of Organic Vapors from Gas Streams,'' in ''Polymeric Gas Separation Membrane,'' D. R. Paul and Y. P. Yampol'skii, Eds., CRC Press, Boca Raton, FL (1994), pp. 353–397.

Baker, R. W., J. G. Wijmans and J. H. Kaschemekat, ''The Design of Membrane Vapor-Gas Separation System,'' J. Membr. Sci. **151**, 55–62 (1998).

Coker, D. T., B. D. Freeman and G. K. Fleming, ''Modeling Multicomponent Gas Separation using Hollow-Fiver Membrane Contactors,'' AIChE J. **44**, (6), 1289–1302 (1998).

Ghosal, K. and B. D. Freeman, ''Gas Separation using Polymer Membrane: An Overview,'' Polymer for Adv. Technol. **5**, 673–697 (1994).

Hinchliffe, A. B. and K. Porter, ''Gas Separation using Membrane. 1. Optimization of the Separation Process using New Cost Parameters,'' Ind. Eng. Chem. Res. **36**, 821–829 (1997).

Jiang, X. and A. Kumar, ''Performance of Silicone-Coated Polymeric Membrane in Separation of Hydrocarbons and Nitrogen Mixtures,'' J. Membr. Sci. **254**, 179–188 (2005).

Jiang, X. and A. Kumar, ''Silicone-Coated Polymeric Membrane for Separation of Hydrocarbons and Nitrogen at Sub-Ambient Temperature,'' J. Membr. Sci. **286**, 285–292 (2006).

Kaldis, S. P., G. C. Kapantaidakis, T. I. Papadopoulos and G. P. Sakellaropoulos, ''Simulation of Binary Gas Separation in Hollow Fiber Asymmetric Membrane by Orthogonal Collocation,'' J. Membr. Sci. **142**, 43–59 (1998).

Kaldis, S. P., G. C. Kapantaidakis and G. P. Sakellaropoulos, ''Simulation of Multicomponent Gas Separation in a Hollow Fiber Membrane by Orthogonal Collocation-Hydrogen Recovery from Refinery Gases,'' J. Membr. Sci. **173**, 61–71 (2000).

Leemann, M., G. Eigenberger and H. Strathmann, ''Vapor Permeation for the Recovery of Organic Solvents from Waste Air Streams: Separation Capacities and Process Optimization,'' J. Membr. Sci. **113**, 313–322 (1996).

Lin, N., E. V. Wagner, B. D. Freeman, L. G. Toy and R. P. Gupta, ''Plasticization-Enhanced Hydrogen Purification using Polymeric Membranes,'' Science, **311**, 639–642 (2006).

Liu, L., A. Chakma and X. Feng, ''Propylene Separation from Nitrogen by Poly(Ether Block Amide) Composite Membranes,'' J. Membr. Sci. **279**, 645–654 (2006).

Mattiott, J. and E. Sorensen, ''A General Approach to Modeling Membrane Modules,'' Chem. Eng. Sci. **58**, 4975–4990 (2003).

Merkel, T. C., V. I. Bondar, K. Nagai, B. D. Freeman and I. Pinnau, ''Gas Sorption, Diffusion, and Permeation in Poly(Dimethylsiloxane),'' J. Poly. Sci. Poly. Phys. **38**, 415–434 (2000).

Nitsche, V., K. Ohlrogge and K. Sturken, ''Separation of Organic Vapors by Means of Membranes,'' Chem. Eng. Technol. **21**, (12), 925–935 (1998).

Pan, C. Y., ''Gas Separation by High-Flux, Asymmetric Hollow-Fiber Membrane,'' AIChE J. **32**, (12), 2020–2027 (1986).

Pinnau, I. and Z. J. He, ''Pure-and Mixed–Gas Permeation Properties of Polydimethylsiloxane for Hydrocarbon/Methane and Hydrocarbon/Hydrogen Separation,'' J. Membr. Sci. **244**, 227–233 (2004).

Shindo, Y., T. Hakuta, H. Yoshitome and H. Inoue, ''Calculation Methods for Multicomponent Gas Separation by Permeation,'' Sep. Sci. Tech. **20**, (5 & 6), 445–459 (1985).

Sridhar, S. and A. A. Khan, ''Simulation Studies for the Separation of Propylene and Propane by Ethylcellulose Membrane,'' J. Membr. Sci. **159**, 209–219 (1999).

Tessendorf, S., R. Gani and M. L. Michelsen, ''Modeling, Simulation and Optimization of Membrane-Based Gas Separation Systems,'' Chem. Eng. Sci. **54**, 943–955 (1999).

Thundyil, M. J. and W. J. Koros, ''Mathematical Modeling of Gas Separation Permeators—for Radial Crossflow, Countercurrent, and Cocurrent Hollow Fiber Membrane Modules,'' J. Membr. Sci. **125**, 275–291 (1997).

Manuscript received February 27, 2007; revised manuscript received August 8, 2007; accepted for publication August 9, 2007.